

Canonical scale separation in 2D incompressible hydrodynamics

Klas Modin

Chalmers University of Technology and University of Gothenburg, Gothenburg,
Sweden

Milo Viviani

Scuola Normale Superiore di Pisa, Pisa,
Italy

(Dated: May 24, 2022)

Characterization of the long-time behavior of an inviscid incompressible fluid evolving on a two-dimensional domain is a long-standing problem in mathematical physics. The motion is described by Euler's equations: a non-linear system with infinitely many conservation laws, yet non-integrable dynamics. In both experiments and numerical simulations, coherent vortex structures, or blobs, typically emerge after some stage of initial mixing. These formations dominate the slow, large-scale dynamics. Nevertheless, fast, small-scale dynamics also persist. Kraichnan, in his classical work, qualitatively describes a direct cascade of enstrophy into smaller scales and a backward cascade of energy into larger scales. Previous attempts to quantitatively model this double cascade are based on filtering-like techniques that enforce separation from the outset. Here we show that Euler's equations possess a natural, intrinsic splitting of the vorticity function. This canonical splitting is remarkable in four ways: (i) it is defined only in terms of the Poisson bracket and the Hamiltonian, (ii) it characterizes steady flows (equilibria), (iii) it genuinely, without imposition, evolves into a separation of scales, thus enabling the quantitative dynamics behind Kraichnan's qualitative description, and (iv) it accounts for the "broken line" in the power law for the energy spectrum (observed in both experiments and numerical simulations). The splitting originates from a quantized version of Euler's equations in combination with a standard quantum-tool: the spectral decomposition of Hermitian matrices. In addition to theoretical insight, the canonical scale separation dynamics might be used as a foundation for stochastic model reduction, where the small scales are modeled by suitable multiplicative noise.

CONTENTS

I. Introduction	1
A. Two-dimensional Euler equations	3
B. Overview of the paper	3
II. Background: quantized Euler equations	4
III. Vorticity splitting for quantized hydrodynamics	4
A. Dynamics of W_s and W_r	5
B. Energy and enstrophy splitting	6
IV. Dynamically emerging scale separation	7
V. Vorticity splitting for classical 2D hydrodynamics	10
VI. Conclusions and outlook	13
Appendix A: Stream function splitting	13
References	13

I. INTRODUCTION

Two-dimensional turbulence is the study of incompressible hydrodynamics at large (including infinite) Reynolds numbers. It is a vibrant field in both mathematics and physics, going back to [Euler \(1757\)](#) who derived, in two and three space dimensions, the equations that since bear his name. Turbulent flows in two space dimensions do not exist as classical fluids in nature. Rather, they constitute basic models of intermediate-scale flows in "almost" two-dimensional (thin)

domains, particularly the atmosphere or ocean (cf. *geophysical hydrodynamics* ([Cullen, 2006](#); [Dolzhansky, 2013](#); [Majda and Wang, 2006](#); [Pedlosky, 2013](#); [Zeitlin, 2018](#))).

The conditions of two-dimensional turbulence can be emulated in experiments, e.g., by a soap film flowing rapidly through a fine comb ([Couder, 1984](#)), or by a conducting fluid confined to a thin layer and driven into turbulence by a temporally varying magnetic field ([Sommeria, 1988](#)). When such a turbulent "quasi-2D" flow is released it self-organizes into blob-like condensates, as depicted for the sphere in [Figure 1](#). Heuristically, the mechanism is driven by merging of equally signed vorticity regions. This merging at large scale is, of course, balanced by fine scale dissipation. The field of two-dimensional turbulence is, in many ways, driven by the quest to understand this scale separation.

As a tool for theoretical progress, [Onsager \(1949\)](#) suggested the framework of statistical mechanics applied to a finite but large number of interacting *point vortices*. These are weak (distributional) solutions of the Euler equations where the vorticity function is described by a sum of weighted Dirac delta functions. Onsager realized that a fixed number of point vortices confined to a finite spatial domain can have energies from $-\infty$ to ∞ and therefore the phase volume function $\nu(E)$ must have an inflection point at some finite energy E^* . At this energy the thermodynamical temperature is zero, as follows from Boltzmann's entropy formula since $\nu(E)$ is strictly monotone. If the energy of a system exceeds E^* , in which case the temperature is negative, then, according to thermo-

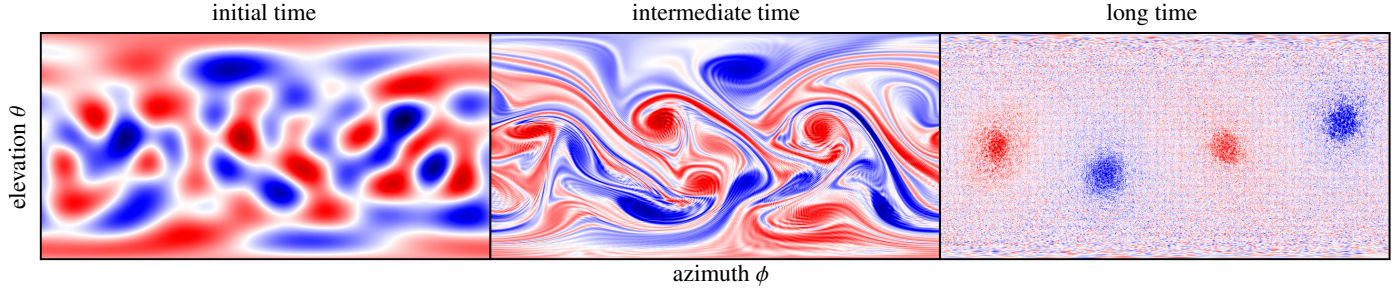


FIG. 1: Evolution of vorticity for Euler's equations on the sphere. Vorticity regions of equal sign undergo merging to form stable, interacting vortex condensates.

dynamics, vortices of the same sign will tend to cluster. Onsager's theory of statistical hydrodynamics thereby predicts vorticity condensation in the turbulent regime—a prominent, although lesser known, part of his legacy (Eyink and Sreenivasan, 2006). On the mathematical side, rigorous results on clustering of point vortices in the negative temperature regime were proved during the 1990s by Caglioti *et al.* (1992, 1995) and by Kiessling (1993), and have fostered much progress (see Marchioro and Pulvirenti (2012) and references therein). On the experimental side, 70 years after Onsager put forward his theory, the conditions of negative temperature 2D point vortex dynamics were experimentally realized in planar Bose-Einstein condensates; as predicted, persisting vortex clusters emerge (Gauthier *et al.*, 2019; Johnstone *et al.*, 2019).

Onsager pointed out that his theory cannot be applied to continuous vorticity fields (corresponding to smooth solutions) and therefore has limited applicability. As a remedy it is natural to look for a statistical theory applicable to continua. One approach is to expand the vorticity field in a Fourier series and then truncate it to obtain a finite dimensional system (Kraichnan, 1975). The truncated system preserves phase volume and quadratic invariants but not higher order invariants (Casimir functions). Another approach, which works for higher order invariants, is to maximize the entropy of a probability distribution of coarse-grained vorticity fields (Miller, 1990; Robert and Sommeria, 1991). All such statistical mechanics based theories rely on the assumption that the dynamics is *ergodic*. Rigorous results on ergodicity are available for 2D Navier-Stokes on a doubly periodic domain with added regular-in-space noise proportional to the square root of the viscosity ν . In this setting there exists a unique stationary measure μ_ν (Kuksin and Shirikyan, 2012, 2017). Furthermore, as $\nu \rightarrow 0$ one obtains a stationary measure μ_0 for the 2D Euler equations, but it may (indeed is expected to) be non-unique (Kuksin and Shirikyan, 2017).

A different strategy is to study the energy spectrum, as in the theory of 3D turbulence by Kolmogorov (1941). Building on that, Kraichnan (1967) showed in his classical work that viscous 2D fluids in forced equilibrium, where energy is fed into the system at an intermediate scale (sometimes called *forced two-dimensional turbulence*), exhibit a forward cascade of entropy into fine scales and at the same time a backward cascade of energy into large scales. Direct numeri-

cal simulation typically support Kraichnan's theory (see Xiao *et al.* (2009) and references therein).

For two-dimensional systems with no energy dissipation at the large scale (so that vortex condensation occurs), numerical simulations eventually settle at a “broken line” energy spectrum with a slope of k^{-3} at the large scale (where k is the wave-number) and then a swift switch at an intermediate scale to a slope between $k^{-5/3}$ and k^{-1} (Boffetta and Ecke, 2012). An approximate $(k^{-3}, k^{-5/3})$ broken line energy spectrum is also observed in zonal and meridional wind measurements on Earth over the scales 3–10,000 km (Nastrom *et al.*, 1984).

To better understand characteristic energy spectra it is natural to impose a splitting of the vorticity field $\omega = \omega_s + \omega_r$ into a large-scale component ω_s and a small-scale component ω_r . Indeed, a wavelet-based vorticity splitting is proposed by Farge *et al.* (1999) and applied to numerical simulation on the periodic square (where condensation occurs) by Chertkov *et al.* (2007). These results (*cf.* Chertkov *et al.* (2007, fig. 1f)) show an energy spectrum slope of k^{-3} for the large scale component (containing one negative and one positive vortex condensate) and of k^{-1} for the intermediate-to-small scale component. Such vorticity decomposition techniques provide powerful methods to better understand energy spectra in two-dimensional turbulence. However, since those methods impose a decomposition of scales from the onset, they are not canonical (they depend on a choice of wavelet basis, as well as on parameters identifying the different scales) and therefore cannot give insights on the mechanisms of vortex condensation and broken line energy spectra.

In this paper we give a new, canonical decomposition of vorticity. With “canonical” we mean parameters-free, determined solely in terms of the data for the two-dimensional Euler equations: the Poisson bracket and the Hamiltonian function (see subsection below). The decomposition has the following properties:

1. $\omega = \omega_s + \omega_r$ is a steady state if and only if $\omega_r = 0$.
2. ω_s and ω_r evolve, by the dynamics of the Euler equations, into a separation of scales, such that ω_s contains the large-scale vortex condensates, whereas ω_r contains small-scale fluctuations.
3. After a short transient time, the energy spectrum slope

of ω_s is k^{-3} and of ω_r is between $k^{-5/3}$ and k^{-1} .

We furthermore identify the individual dynamics of ω_s and ω_r , thereby enabling a study of the mechanisms behind vortex condensation and broken line energy spectra, including the interaction between these mechanisms. Before explaining the decomposition we give a brief presentation of the equations under study and their invariants.

A. Two-dimensional Euler equations

We are interested in Euler's equations for a homogeneous, inviscid, and incompressible fluid confined to a two-dimensional closed surface. Throughout the paper we take the surface to be the unit sphere \mathbb{S}^2 as it makes our arguments more explicit and enables numerical simulations. However, most concepts are transferable to arbitrary closed surfaces (in particular to the flat torus, which is the most studied example in the literature, albeit less relevant than the sphere in applications).

In vorticity formulation, Euler's equations on \mathbb{S}^2 are

$$\dot{\omega} = \{\psi, \omega\}, \quad \Delta\psi = \omega, \quad (1)$$

where $\{\cdot, \cdot\}$ is the Poisson bracket, ω is the vorticity function of the fluid, related to the fluid velocity \mathbf{v} via $\omega = \text{curl } \mathbf{v}$, and ψ is the stream function, related to the vorticity function via the Laplace-Beltrami operator Δ . Geometrically, the equations (1) constitute a *Lie-Poisson system* on the dual of the infinite-dimensional Lie algebra of divergence free vector fields (cf. Arnold and Khesin (1998)). This infinite-dimensional Hamiltonian system has an infinite number of conservation laws: total energy (which is also the Hamiltonian function)

$$H = -\frac{1}{2} \int_{\mathbb{S}^2} \psi \omega,$$

total angular momentum

$$\mathbf{L} = \int_{\mathbb{S}^2} \omega \mathbf{n}, \quad \mathbf{n} \text{ unit normal on } \mathbb{S}^2,$$

and Casimir functions

$$C_f(\omega) = \int_{\mathbb{S}^2} f(\omega), \quad \text{for any smooth } f: \mathbb{R} \rightarrow \mathbb{R}.$$

These conservation laws are fundamental for the long-time behavior. In particular, the presence of an infinite number of Casimir functions is what sets two- and three-dimensional fluids apart.

Remark I.1. The statistical hydrodynamics theories by Miller, Robert, and Sommeria mentioned above have been worked out on \mathbb{S}^2 by Herbert (2013) in a setting that uses three of the conservation laws: momentum \mathbf{L} , energy H , and enstrophy $C_2 := \int \omega^2$. The calculations by Herbert predict a

near steady state resulting in a superposition of a quadrupole and a dipole. These predictions are challenged by Casimir preserving numerical simulations on \mathbb{S}^2 for which the generic behavior is formation of three (if the momentum is intermediate) or four (if the momentum is small) vortex blob condensates which interact in a non-stationary but integrable fashion (Modin and Viviani, 2020a).

The canonical scale separation of ω is established through a finite-dimensional approximation of the Euler equations (1) obtained via quantization. We now give an outline of the paper which also serves as a summary of how the quantized Euler equations give rise to the canonical vorticity splitting.

B. Overview of the paper

Quantized Euler equations are obtained from the vorticity formulation of the Euler equations. Applying quantization (more precisely Berezin-Toeplitz quantization of compact Kähler manifolds), one replaces the space of (smooth) vorticity functions with the matrix algebra $\mathfrak{su}(N)$, while the Poisson bracket is replaced by the matrix commutator. N is thought of as the spatial discretization parameter, so that $N \rightarrow \infty$ as $\hbar \rightarrow 0$. We present details on the quantized Euler equations in section II.

There are at least two advantages of quantized Euler equations. First, they yield a spatial discretization that preserve all the underlying geometry of the Euler equations: the Hamiltonian structure (more precisely the Lie-Poisson structure) and the conservation laws (Casimirs, Hamiltonian, and momentum). Combined with a symplectic time-integration scheme this yields a fully structure preserving numerical method (Modin and Viviani, 2020a). Second, complicated topological or geometrical properties of the Euler equations can be described in terms of standard tools from linear algebra and matrix Lie groups. Indeed, our splitting of the quantized vorticity naturally arise from the standard spectral decomposition of Hermitian matrices applied to the quantized stream function. This splitting has a precise geometric meaning in terms of Lie algebras, but also a dynamical interpretation as the steady and unsteady vorticity components. The details are given in section III.

In section IV we discuss properties of the canonical vortex splitting. The main point is the dynamical convergence of the splitting into a separation of scales. Indeed, separation of scales in the vorticity energy profile, explaining the broken line spectrum, is completely captured by our splitting. We give arguments supported by numerical simulations for the mechanism. In section V we translate our results from the quantized to the classical Euler equations, thus interpreting the matrix-based results in a fluid dynamical formulation. This work sets the foundation for an L^∞ -based mathematical theory of canonical vorticity splitting.

II. BACKGROUND: QUANTIZED EULER EQUATIONS

In this section we present a quantized version of Euler's equations, first introduced by Zeitlin (1991, 2004). The model, sometimes called *consistent truncation* or *quantized Euler equations*, relies on quantization of the infinite-dimensional Poisson algebra of the smooth functions $C^\infty(\mathbb{S}^2)$. Recall that the Poisson bracket $\{f, g\}$ for $x \in \mathbb{S}^2$ and $f, g \in C^\infty(\mathbb{S}^2)$ is the function given by

$$\{f, g\}(x) = x \cdot (\nabla f \times \nabla g).$$

Quantization (in the context here) means to find a projection from smooth functions to the Lie algebra of skew-Hermitian matrices $\Pi_N: C^\infty(\mathbb{S}^2) \rightarrow \mathfrak{su}(N)$ such that the Poisson bracket under this map is approximated by the matrix commutator. This type of quantization, called *Berezin-Toeplitz quantization* (cf. Schlichenmaier (2001)), is applicable to compact Kähler manifolds. The classical limit correspond to $N \rightarrow \infty$. Boremann *et al.* (1994) showed that there exists a basis of the Lie algebra $\mathfrak{su}(N)$, such that its structure constant converges to those of $C^\infty(\mathbb{S}^2)$ expressed in the spherical harmonics basis. More specifically, if Y_{lm} denote the classical spherical harmonics basis then, for any $N > 1$, there exists a basis of $\mathfrak{su}(N)$, denoted T_{lm}^N for $l = 1, \dots, N$, such that in the operator norm and for $N \rightarrow \infty$ we have

- $\Pi_N f - \Pi_N g \rightarrow 0$ implies $f = g$,
- $\Pi_N \{f, g\} = N^{3/2} [\Pi_N f, \Pi_N g] + O(1/N)$,
- $\Pi_N Y_{lm} = T_{lm}^N$.

From the classical Euler equations in vorticity formulation (1) we then get the corresponding quantized Euler equations

$$\dot{W} = [P, W], \quad \Delta_N P = W, \quad (2)$$

where $W \in \mathfrak{su}(N)$ is the *vorticity matrix*, $P \in \mathfrak{su}(N)$ is the *stream matrix*, and Δ_N is the *quantized Laplacian* given by Hoppe and Yau (1998).

The quantized Euler equations (2) have been studied in various contexts, primarily on the flat torus (Abramov and Majda, 2003; McLachlan, 1993; Zeitlin, 1991), but more recently also on the sphere (Modin and Viviani, 2020a; Zeitlin, 2004).¹ Their main feature is that they preserve the rich geometry in phase space of the classical equations (1), i.e., the Lie-Poisson structure. In turn, this implies conservation of total energy $H(W) = \text{Tr}(PW)/2$, (quantized) Casimirs $C_k(W) = \text{Tr}(W^k)$,

and angular momentum $\mathbf{L} = (L_x, L_y, L_z)$ (see Modin and Viviani (2020a) for details). No conventional spatial discretization of the Euler equations preserve all these properties.

In previous work by Modin and Viviani (2020a,c) we develop a fully Lie-Poisson preserving numerical method for the quantized Euler equations on the sphere and we use this method to study the long-time behavior. As previously also observed by Dritschel *et al.* (2015), the numerical results give strong evidence against the predictions of statistical mechanics based theories (cf. Bouchet and Venaille (2012)). Rather, the results suggest the existence of near-integrable parts of phase space that act as barriers for the statistical predictions to be reached. Those near integrable solutions take the form of interacting vortex blobs (3 or 4 depending on the total angular momentum), perfectly reflecting integrability results for point vortex dynamics on the sphere (cf. Modin and Viviani (2020b)).

Working with the quantized Euler equations, a novel notion emerged: more than a spatial discretization, the quantized Euler equations themselves provide new tools for studying the long-time behavior of 2D hydrodynamics. Those tools include, in particular, Lie theory for $\mathfrak{su}(N)$, which is exceptionally well understood, for example from the point of Kähler geometry, quantum theory, representation theory, and linear algebra. In particular, looking at the quantized Euler equations through the lens of Lie algebra theory it is natural to split the vorticity matrix by projection onto the *stabilizer* of P : the underpinning of this paper. This splitting captures the dynamics of vortex condensation and scale separation, related to the theory of Kraichnan (1967) of an inverse energy cascade: it splits the dynamics into a *dynamically passive* and a *dynamically active* part.

III. VORTICITY SPLITTING FOR QUANTIZED HYDRODYNAMICS

In this section we present and discuss canonical vorticity splitting for the quantized Euler equations. With “canonical” we mean here that the splitting only depend on the Lie algebra structure (and of course on the vorticity matrix W and the stream matrix P governing the dynamics). In particular, it does not require any *ad hoc* choice of scale as previous methods do – the separation of scales is a result of the dynamics itself.

Consider again the quantized Euler equations (2). Recall that the canonical inner product on $\mathfrak{su}(N)$ is minus the Killing form. In the standard matrix representation of $\mathfrak{su}(N)$ it coincides with the Frobenius norm. We now define a splitting of the vorticity matrix

$$W = W_s + W_r \quad (3)$$

by setting W_s to be the orthogonal projection of W onto the *stabilizer algebra* of the stream matrix P

$$\text{stab}_P = \{A \in \mathfrak{su}(N) \mid [A, P] = 0\}.$$

¹ Although the spherical setting is more complicated to work with (due to the appearance of Wigner-3j symbols of very high order), the quantized Euler equations actually works *better* on the sphere than on the torus. There is a deep geometrical reason for this: quantization on the sphere exactly preserves the $\text{SO}(3)$ symmetry of the sphere, whereas the corresponding translational symmetry in the quantization of the torus is only approximately captured.

Let us assume now P to be *generic* so that all its eigenvalues are distinct. Then stab_P is equivalently given by

$$\text{stab}_P = \{A \in \mathfrak{su}(N) \mid A, P \text{ simultaneously diagonalizable}\}.$$

Hence, in this case W_s is obtained via the spectral decomposition: first find $E \in \text{SU}(N)$ which diagonalizes P , i.e., $E^\dagger P E = \Lambda$, then set $\Pi_P : \mathfrak{su}(N) \rightarrow \text{stab}_P$ as

$$W_s := \Pi_P(W) = E \text{diag}(E^\dagger W E) E^\dagger.$$

With respect to the canonical vorticity splitting (3), the quantized Euler equations (2) can be written

$$\dot{W} = [P, W_r].$$

Notice that the variable W_s is dynamically “inactive”: $W = W_s + W_r$ is a steady solution (equilibrium) if and only if $W_r = 0$, so the dynamics is “driven by” the residual part W_r .

A. Dynamics of W_s and W_r

To obtain insight on the canonical splitting (3) we shall work out the dynamics fully in terms of W_s and W_r . To this end, consider first a general matrix flow on $\mathfrak{su}(N)$ of the form

$$\dot{P} = F(P), \quad (4)$$

for some smooth vector field F on $\mathfrak{su}(N)$. Let $E \in \text{SU}(N)$ and $\Lambda \in \text{diag}_N$ be an eigenbasis and the corresponding eigenvalues of P . We shall determine the evolution of E and Λ . It is known that $\mathfrak{su}(N)$ is foliated into (co-adjoint) orbits (cf. Kirillov (2004)) given by

$$O_P = \{Q = U P U^\dagger \mid U \in \text{SU}(N)\}.$$

In the generic case (all eigenvalues of P distinct), the tangent space $T_P O_P$ is spanned by $\{e_k e_l^\dagger\}_{k \neq l}$,² where $E = [e_1, \dots, e_N]$ is the orthonormal eigenbasis of P . If we take the orthogonal directions $\text{span}\{e_k e_k^\dagger\}$ of the tangent spaces (with respect to the canonical bi-invariant inner product), we obtain the linear subspace of matrices in $\mathfrak{su}(N)$ sharing the same eigenbasis (i.e., they are simultaneously diagonalizable). In the language of Lie algebras, it corresponds to the *isotropy algebra* of P . Thus we have

$$\Pi_P : \mathfrak{su}(N) \rightarrow \text{stab}_P \quad \text{and} \quad \Pi_P^\perp := \text{Id} - \Pi_P : \mathfrak{su}(N) \rightarrow \text{stab}_P^\perp$$

corresponding respectively to decomposition in the basis $\{e_k e_k^\dagger\}_k$ and $\{e_k e_l^\dagger\}_{k \neq l}$. Notice, as expected, that neither Π_P nor Π_P^\perp depend on the eigenvalues of P , only the eigenbasis.

We can now write the equation (4) as

$$\dot{P} = \Pi_P F(P) + \Pi_P^\perp F(P)$$

The first part of the flow changes the eigenbasis but not the eigenvalues and vice versa. The question is: what is the generator of $P \mapsto \Pi_P^\perp F(P)$? Since it is isospectral it should be of the form $P \mapsto [B(P), P]$ for some $B(P) \in \mathfrak{su}(N)$. Let us denote $X = F(P)$. It is then straightforward to check that if all the eigenvalues p_1, \dots, p_N of P are different, then

$$\begin{aligned} \Pi_P^\perp X &= \sum_{k \neq l} x_{kl} e_k e_l^\dagger = \sum_{k \neq l} (p_k - p_l) b_{kl} e_k e_l^\dagger \\ &= \left[\sum_{k \neq l} b_{kl} e_k e_l^\dagger, P \right] = [B, P] \end{aligned}$$

where x_{kl} are the components of X in the basis E , and $b_{kl} := x_{kl}/(p_k - p_l)$. Thus, in the generic case we can construct the generator $B(P)$ from the eigenvalues p_1, \dots, p_N and the eigenbasis e_1, \dots, e_N of P . This allows us to write equation (4) in terms of the eigenvalues and eigenbasis of P as

$$\begin{aligned} \dot{p}_k &= e_k^\dagger X e_k, & X &= F\left(\sum_{k=1}^N p_k e_k e_k^\dagger\right) \\ \dot{e}_k &= B e_k, & B &= \sum_{k \neq l} \frac{e_k^\dagger X e_l}{p_k - p_l} e_k e_l^\dagger. \end{aligned}$$

Remark 1. The evolution of the eigenbasis of P plays a major role in the variation of the energy metric $H(P) = 1/2 \text{Tr}(\Delta_N P P)$. Using that

$$\Delta_N P = [X_0, [X_0, P]] + \frac{1}{2} [X_-, [X_+, P]] + \frac{1}{2} [X_+, [X_-, P]]$$

we see that

$$E^\dagger \Delta_N P E = [Y_0, [Y_0, \Lambda_P]] + \frac{1}{2} [Y_-, [Y_+, \Lambda_P]] + \frac{1}{2} [Y_+, [Y_-, \Lambda_P]]$$

where $Y_i = E^\dagger X_i E$, i.e., the matrices X_i expressed in the eigenbasis E . Thus, the Y_i are also transported by the generator B , so they can be thought of as advected quantities

$$\dot{Y}_i = \pm [B, Y_i].$$

Since $\{X_i\}$ are generators for a representation of $\mathfrak{su}(2)$ in $\mathfrak{su}(N)$ corresponding to the isometries of the sphere (see Hoppe and Yau (1998)), deforming $\{X_i\}$ to $\{Y_i\}$ give another representation that corresponds to deforming the spherical metric via a symplectomorphism. Notice, however, that the Y_i are complicated from the start (since E is complicated from the start). In fact, working in the eigenbasis of P corresponds for the classical Euler equations to use coordinates where the stream function ψ is zonal (constant along longitudes). Of course, such coordinates can never be smooth, so the analogy must necessarily be taken in a weak sense.

Remark 2. The matrices $E_{kk} = i e_k e_k^\dagger$ form an orthonormal basis for stab_P (in the generic case). A key insight is that these matrices are quantized analogs of the level sets of the stream function ψ . Indeed, up to small oscillations resembling

² Here we assume P generic, i.e., with all the eigenvalues distinct.

a wavelet basis, the interpretation of the spectral decomposition of P is that its eigenvalues correspond to the values that the respective stream function takes, whereas its eigenvectors (or the matrices E_{kk}) correspond to the connected components of the level curves of the respective stream function as depicted in [Figure 2](#). This is of course again in a weak sense.

Let us now apply the machinery to obtain the dynamics of W_s and W_r . By the definition of W_s

$$\begin{aligned}\dot{W}_s &= \frac{d}{dt} \left(E \text{diag}(E^\dagger W E) E^\dagger \right) \\ &= [\dot{E} E^\dagger, W_s] - \Pi_P([\dot{E} E^\dagger, W_r]),\end{aligned}$$

where we have used that $\Pi_P(\dot{W}) = 0$ and $\dot{E} E^\dagger = -E \dot{E}^\dagger$. This dynamics is close to that of P

$$\dot{P} = [\dot{E} E^\dagger, P] + E \dot{D}_P E^\dagger.$$

Hence, a formula for $\dot{E} E^\dagger$ is needed. To this end, we know that the dynamics of P can be orthogonally decomposed as

$$\dot{P} = \Pi_P^\perp(\Delta_N^{-1}[P, \Delta P]) + \Pi_P(\Delta_N^{-1}[P, \Delta P]),$$

so it follows that

$$[\dot{E} E^\dagger, P] = \Pi_P^\perp(\Delta_N^{-1}[P, \Delta P]).$$

Notice that $\dot{E} E^\dagger$ can be taken in stab_P^\perp . In fact, the dynamics of W_s remains the same for any $\dot{E} E^\dagger + S$, where $S \in \text{stab}_P$. The map:

$$[\cdot, P] : \text{stab}_P^\perp \rightarrow \text{stab}_P^\perp$$

is invertible so $\dot{E} E^\dagger$ is uniquely determined in stab_P^\perp . In conclusion we have derived the following result for the dynamics of W_s and W_r .

Theorem 1. *Let $W = W(t)$ be a solution to the quantized Euler equations (2) and W_s, W_r respectively be the orthogonal projections of W onto stab_P and its orthogonal complement. Then, W_s and W_r satisfy the following system of equations*

$$\begin{aligned}\dot{W}_s &= [B, W_s] - \Pi_P[B, W_r] \\ \dot{W}_r &= -[B, W_s] + \Pi_P[B, W_r] + [P, W_r],\end{aligned}$$

where $P = \Delta_N^{-1}(W_s + W_r)$ and B is the unique solution in stab_P^\perp to

$$[B, P] = \Pi_P^\perp \Delta_N^{-1}[P, W_r]. \quad (5)$$

From Theorem 1 we can deduce properties of W_s and W_r . First notice that if $W_r = 0$ then $B = 0$. Indeed, if $W_r = 0$ then $B \in \text{stab}_P \cap \text{stab}_P^\perp$ so $B = 0$, and conversely if $B = 0$ then $\dot{W}_s = 0$ and $\dot{W}_r = [\Delta_N^{-1}(W_s + W_r), W_r]$. Hence, in that case W_s plays the role of a fixed topography for W_r , which satisfies a Euler-type equation. From equation (5) we deduce that $B = 0$ also implies

$$\text{Tr}(\Delta_N^{-1} W_s [\Delta_N^{-1} W_r, W_r]) = 0. \quad (6)$$

Another observation is that if $[B, W_s] = 0$ then $B = 0$ so $\dot{W}_s = 0$, and vice versa if $\Pi_P[B, W_r] = 0$ then again equation (6) holds. This means that it is possible to have an evolution of the eigenvectors of P without any change of the eigenvalues, but not the other way around.

B. Energy and enstrophy splitting

Let us now look at how the energy and the enstrophy are related to the canonical splitting (3). By definition, the energy (corresponding to the *energy norm*) is

$$\begin{aligned}H(W) &= \frac{1}{2} \text{Tr}(\Delta_N^{-1}(W_s + W_r) W_s) \\ &= \frac{1}{2} \text{Tr}(\Delta_N^{-1}(W_s) W_s) - \frac{1}{2} \text{Tr}(\Delta_N^{-1}(W_r) W_r)\end{aligned}$$

and the enstrophy (corresponding to the *enstrophy norm*) is

$$E(W) = -\text{Tr}(W_s^2) - \text{Tr}(W_r^2).$$

Hence, we have the interesting relations

$$\begin{aligned}H(W) &= H(W_s) - H(W_r) \\ E(W) &= E(W_s) + E(W_r).\end{aligned} \quad (7)$$

Notice that $W_s = 0$ if and only $W = 0$ (since $\sqrt{H(\cdot)}$ is a norm). Moreover, if $W \neq 0$ then

$$0 < H(W) \leq H(W_s) < E(W_s) \leq E(W).$$

That the energy $H(W_s)$ is larger than the energy $H(W)$ can be interpreted in the following way: it is possible for the energy of W_s and W_r to decrease simultaneously (this is, in fact, exactly what happens as we shall see), but if the enstrophy of W_s is decreasing then the enstrophy of W_r must increase. This corresponds to the description of [Kraichnan \(1967\)](#) of an inverse energy cascade and a forward enstrophy cascade.

It is possible to represent the energy-enstrophy splitting (7) in a more geometric way. The first equation of (7) tells that W and W_r are orthogonal in the energy norm, whereas the second equation says that W_s and W_r are orthogonal in the enstrophy norm. Let us take the (W, W_r) -plane, and let $H_r = H(W_r)$ and $H_0 = H(W)$. Then, as $W_r = (0, \sqrt{H_r})$ and $W = (\sqrt{H_0}, 0)$ in this plane, the energy norm is the identity matrix on \mathbb{R}^2 . We want to express the enstrophy norm with respect the energy norm. Let us first observe that $W_s = (\sqrt{H_0}, -\sqrt{H_r})$. Then, the positive definite matrix G for the enstrophy inner product restricted to the (W, W_r) -plane can be written as $G = C^\top C$, where $C: \mathbb{R}^2 \rightarrow \mathbb{R}^2$ is such that $C(0, \sqrt{H_r})^\top = (0, \sqrt{E_0} \sin \alpha)^\top$ and $C(\sqrt{H_0}, 0)^\top = \sqrt{E_0}(\cos \alpha, \sin \alpha)^\top$, where α is the angle between W and W_s in the enstrophy norm and $E_0 = E(W)$. Then we have

$$G = \begin{bmatrix} \frac{E_0}{H_0} & \frac{E_0}{\sqrt{H_r} \sqrt{H_0}} \sin^2 \alpha \\ \frac{E_0}{\sqrt{H_r} \sqrt{H_0}} \sin^2 \alpha & \frac{E_0}{H_r} \sin^2 \alpha \end{bmatrix},$$

in the (W, W_r) -plane. We can derive the following inequalities:

$$\begin{aligned}H_r &\leq E_r = E_0 \sin^2 \alpha \\ N^4 H_r &\geq E_r = E_0 \sin^2 \alpha.\end{aligned}$$

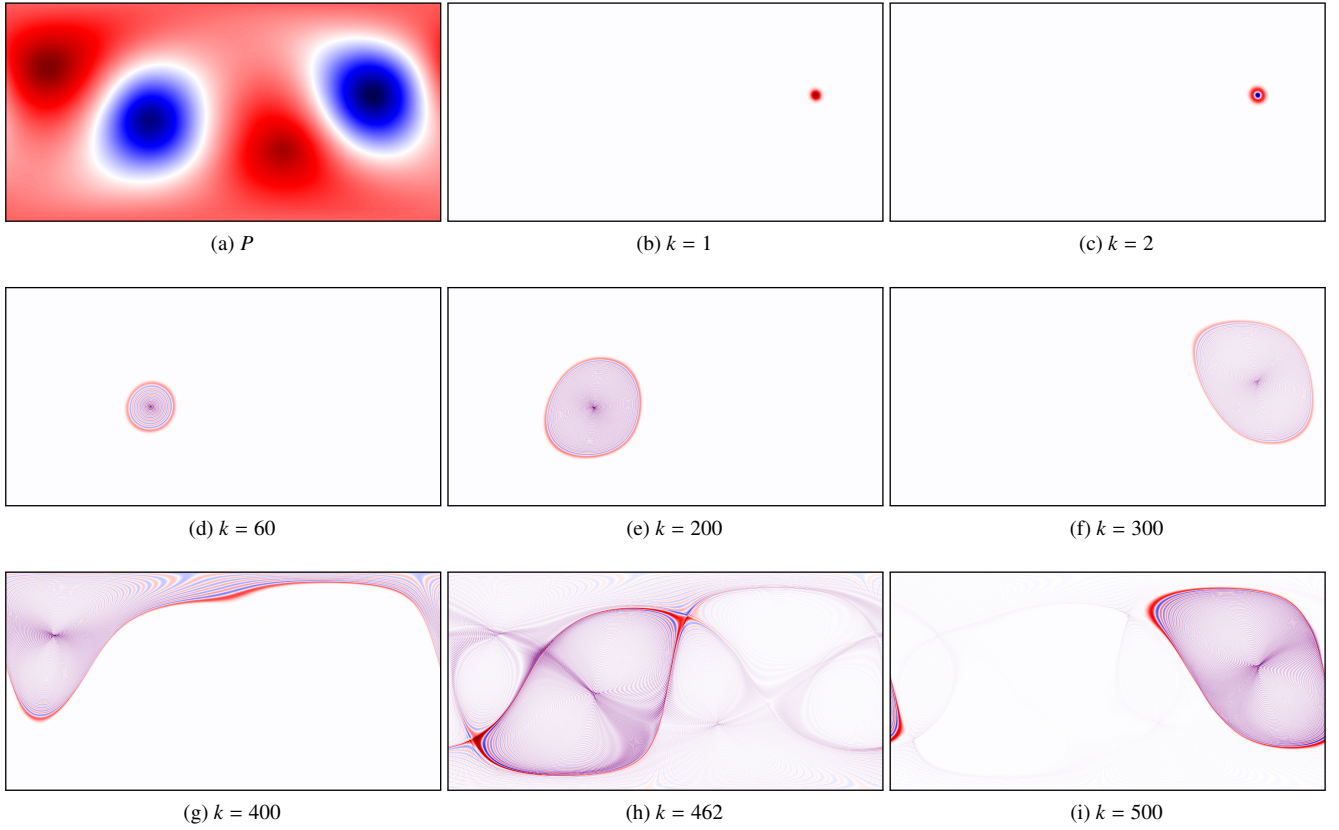


FIG. 2: The basis elements $E_{kk} = ie_k e_k^\dagger$ for the eigenbasis of P for various values of k . The eigenvector e_k is the quantized analog of a level-set of the stream function where the value is given by the eigenvalue p_k . As one can expect, this analogy breaks for level-sets that have bifurcations, as depicted in sub-figure (h).

Hence, if $\sin \alpha \neq 0$ then

$$\frac{E_0}{N^4} \leq \frac{H_r}{\sin^2 \alpha} \leq E_0.$$

We see that in the limit for $N \rightarrow \infty$ the ratio $\frac{\sin^2 \alpha}{H_r}$ is potentially unbounded. Indeed, it could happen that the enstrophy norm of W_r is always far from being zero, whereas its energy norm goes to zero. This corresponds to W_r being shifted towards small scales while not decreasing its enstrophy.

IV. DYNAMICALLY EMERGING SCALE SEPARATION

In this section we show that the canonical vorticity splitting (3) capture the dynamics of the scale separation typical in 2D turbulence. The approach is a combination of numerical and theoretical evidence. As already pointed out, one main motivation for studying the vorticity splitting in the W_s and W_r component is that the unsteadiness of the fluid can be precisely understood in terms of non-vanishing of W_r . Moreover, to derive W_s and W_r we do not rely on any knowledge of the Fourier decomposition or the values of W . From an analytical point of view, W_s represents a projection of W onto a

smoother subspace. Indeed, the relation via the Laplace operator between P and W says that P admits, in general, two more spatial derivatives than W . Hence, since W_s is related to P via a polynomial relationship, W_s is in general more regular than W . Vice versa, W_r contains the rougher part of W . The tempting interpretation is that W_s represents the low-dimensional, large-scale dynamics, whereas W_r represents the noisy, small-scale dynamics. To assess this conjecture, we consider first numerical simulation with smooth, vanishing momentum initial data, depicted in Figure 3(a).³

In Figure 3 the vorticity fields for W , W_s and W_r are shown at $t = 0$ and $t = t_{end} \approx 100$. As expected, after some time of initial mixing the large scales of the vorticity are all contained in the smooth field W_s , whereas W_r contains the small-scale fluctuations. In Figure 5 the evolution of the energy and enstrophy of W_s and W_r are shown: notice that E_r increases whereas H_r decreases in accordance with Kraichnan's inverse energy cascade. In Figure 4(a) the field corresponding to B at $t = t_{end}$ is shown, and the relation between the values taken by

³ The same initial data were previously used by Dritschel *et al.* (2015) and by Modin and Viviani (2020a).

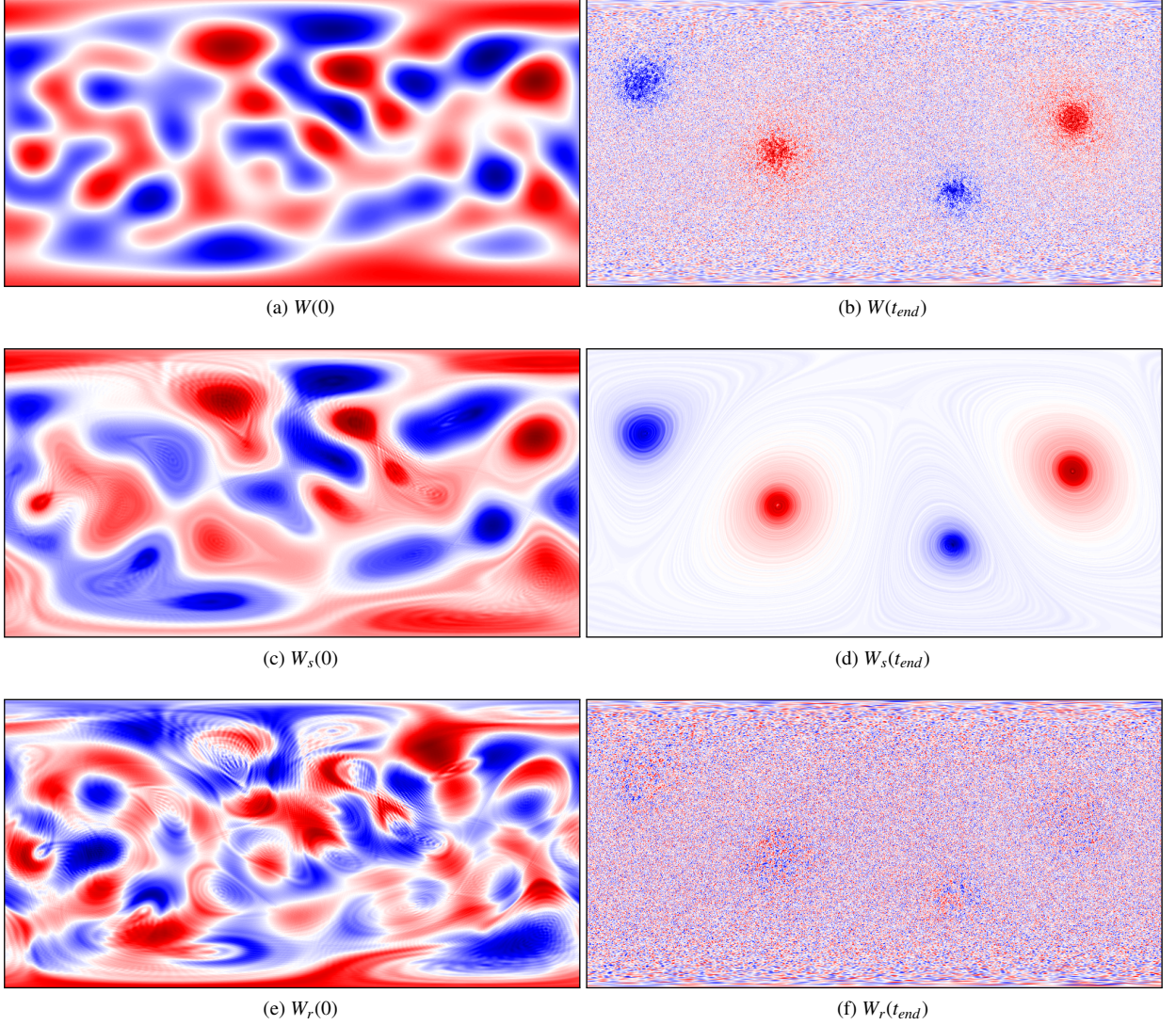


FIG. 3: The fields W , W_s and W_r at $t = 0$ and $t = t_{end}$ in a simulation where four blobs emerge. Initially W_s and W_r are similar in nature, but they evolve so that W_s contains the large-scale condensates whereas W_r contains the small-scale fluctuations.

P and W_s is shown in Figure 4(b).

Notice that B takes its largest values along “boundaries” of the four condensates. This is expected: recall that B is singular at multiple eigenvalues of P . Since eigenvalues correspond to field values, and eigenvectors correspond to level-sets, we can expect B to be large nearby level-sets of the stream function where its values are changing slowly. This happens (i) at extremal points, and (ii) at the boundaries between the condensates. Now, at an extremal point the singularity is cancelled by the numerator, leaving only the shadow of a “star shape” (which we consider a quantum effect). At the boundaries, however, it is not cancelled, which explains the large values there. Furthermore, notice that the boundaries are setup in such a way that vortex condensates of equal sign only meet at a point. Indeed, B has two saddle points corresponding to the bifurcations appearing in Figure 4(b). Thus, these branches

correspond to the four condensates. Clearly, this diagram is not the graph of a function which implies that a functional relation between W_s and P can only be local in space.

The scale separation of the vorticity is even clearer in the spectral domain. Figure 6 contains energy spectra for the vorticity fields corresponding to W , W_s , and W_r at $t = t_{end}$. The energy level $H(l)$, corresponding to the wave-number $l = 1, \dots, N$, contains the energy of the modes with respect to the harmonics Y_{lm} , for $m = -l, \dots, l$. We notice that the energy spectrum of W is similar in nature to the one obtain in (Boffetta and Ecke, 2012). We see that the “broken line” slope in the energy spectrum of W originate from an l^{-3} slope of W_s and an l^{-1} slope of W_r . Thus, the vorticity splitting yields a scale separation of the vorticity field exactly reflecting the broken line spectra previously observed in numerical simulations and empirical observations.

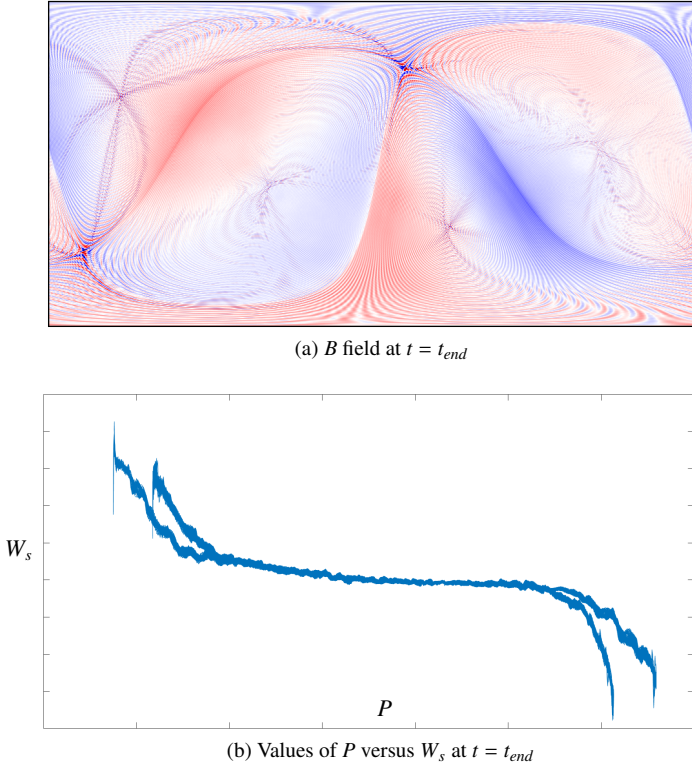


FIG. 4: The B field (a) and the values of P versus W_s in the simulation where four blobs emerge. The B field divides the phase space into four regions marked by the borders between the vortex condensates. These four regions are reflected in the four branches in sub-figure (b).

Next we consider a simulation where three vortex blobs emerge (the formation of such structures on the sphere from initial data with non-vanishing momentum were predicted and demonstrated by [Modin and Viviani \(2020a\)](#), corresponding to integrability of low-dimensional point-vortex dynamics which acts as a blockade for ergodicity in phase space). In [Figure 7](#) the three vorticity fields W, W_s , and W_r are shown at $t = 0$ and $t = t_{\text{end}} \sim 10^2 s$. As before, the large scales of the vorticity are contained in the smooth field W_s whereas W_r swiftly develop into noisy fluctuations.

The field B at $t = t_{\text{end}}$ is depicted in [Figure 8\(a\)](#), and the relation between the values of P and W_s in [Figure 8\(b\)](#). In contrast with [Figure 4](#), notice that there is only one saddle point, and correspondingly only a single bifurcation appearing in [Figure 8\(b\)](#). As predicted, it is clear from [Figures 4-8](#) that the number of blobs correspond to the saddle points of B . The scale separation of the vorticity is again evident looking at the energy spectrum of W . In [Figure IV](#) energy spectra are given for the three vorticity fields W, W_s , and W_r at $t = t_{\text{end}}$. The results are analogous to those in [Figure 6](#).

Finally, we remark that the projection $\Pi_P : \mathfrak{su}(N) \rightarrow \text{stab}_P$ has rank N (in the generic case). Hence, the dynamics of W_s in the moving frame E_{kk} can be described by only N components, i.e., its eigenvalues. Therefore, the vorticity splitting

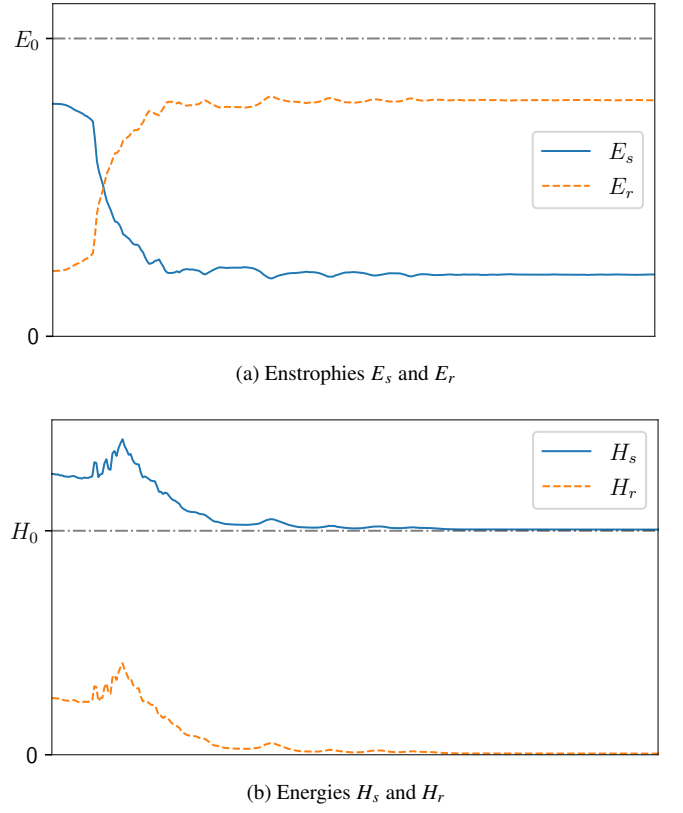


FIG. 5: Evolution of the energy and estrophy of W_s and W_r respectively for the simulation where four blobs emerge. The energy of W_r decays almost to zero, so that almost all the energy is contained in W_s (reflecting the inverse energy cascade). On the other hand, the enstrophy of W_r increases over time (reflecting the forward enstrophy cascade).

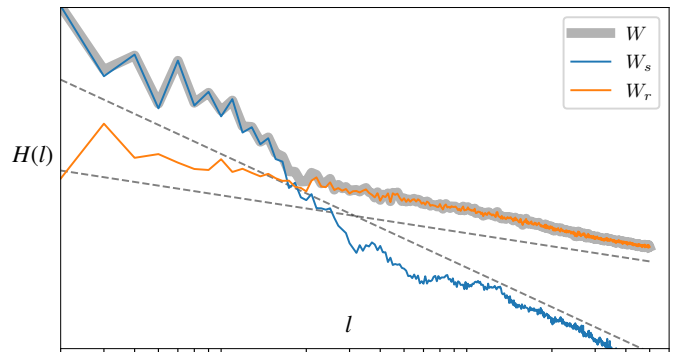


FIG. 6: Energy spectrum in log-log scale for W, W_s , and W_r at $t = t_{\text{end}}$ for the simulation where four blobs emerge. The dashed lines indicate the slopes l^{-3} and l^{-1} .

can be also interpreted as reduced dynamics.

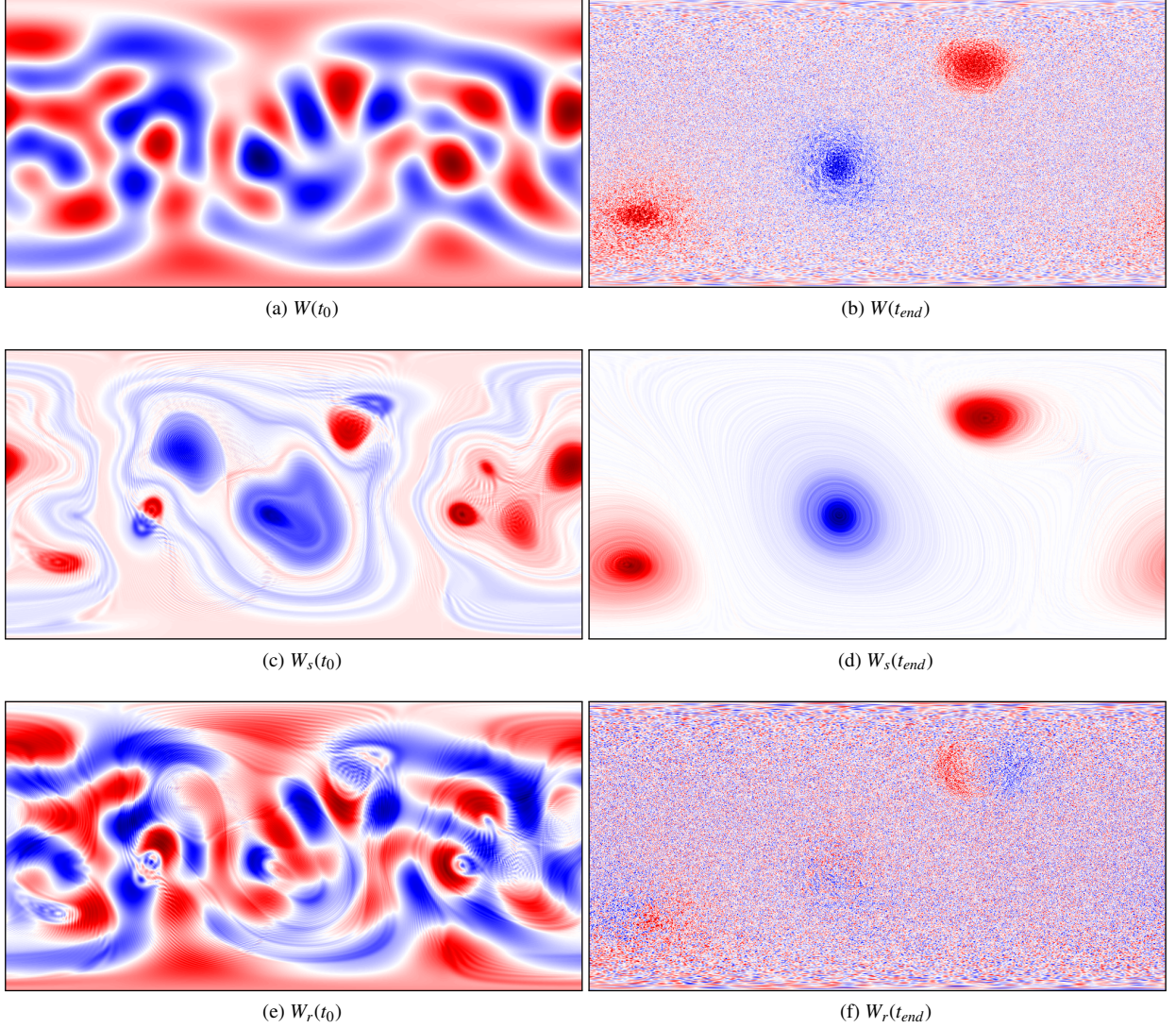


FIG. 7: The fields for the vorticity matrices W , W_s and W_r at $t = 0$ and $t = t_{end}$ for the simulation where three blobs emerge.

V. VORTICITY SPLITTING FOR CLASSICAL 2D HYDRODYNAMICS

In this section we return to the classical Euler equations

$$\dot{\omega} = \{\psi, \omega\}, \quad \Delta\psi = \omega. \quad (8)$$

To define the analog of the quantized vorticity splitting, we have to understand equations (8) in the weak sense. Indeed, in general the analog of the projections Π_P and Π_P^\perp cannot preserve the smoothness of ω . However, they are still continuous with operator norm one, from $C^0(\mathbb{S}^2)$ to $L^p(\mathbb{S}^2)$, for any $p \in [1, \infty]$. Hence, by density of the continuous functions in $L^p(\mathbb{S}^2)$, $p \in [1, \infty)$ we can extend Π_ψ, Π_ψ^\perp to continuous operator to $L^\infty(\mathbb{S}^2)$. This result fits well with the global well-posedness of equations (8), which precisely requires a vorticity function in L^∞ (Marchioro and Pulvirenti, 2012; Yudovich, 1963).

Let us first define the right hand side of equations (8) in the weak sense. For any $p > 2$, if $\omega \in L^p(\mathbb{S}^2)$ then $\psi \in W^{2,p}(\mathbb{S}^2) \subset C^1(\mathbb{S}^2)$. We define the weak Poisson bracket as

$$\int_{\mathbb{S}^2} \{\psi, \omega\} \phi = - \int_{\mathbb{S}^2} \omega \{\psi, \phi\},$$

for any test function $\phi \in C^\infty(\mathbb{S}^2)$. We can now define the stabilizer of ψ as

$$\text{stab}_\psi := \{f \in L^2(\mathbb{S}^2) \mid \{f, \psi\} = 0\}.$$

Next we want to define the projection Π_ψ onto stab_ψ . One issue is that the stabilizer of ψ is not closed in the L^2 topology. However, for continuous functions it is possible to define a projector which minimizes the L^2 distance from stab_ψ . We first make the following assumption on the critical points of ψ .

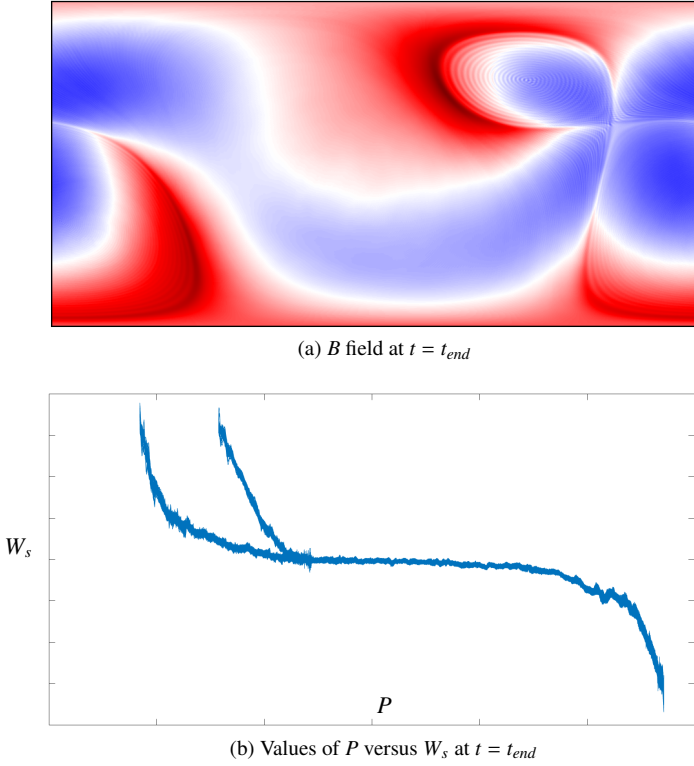


FIG. 8: The B field (a) and the values of P versus W_s (b) in the simulation where three blobs emerge. These three blobs reflect the three branches in sub-figure (b).

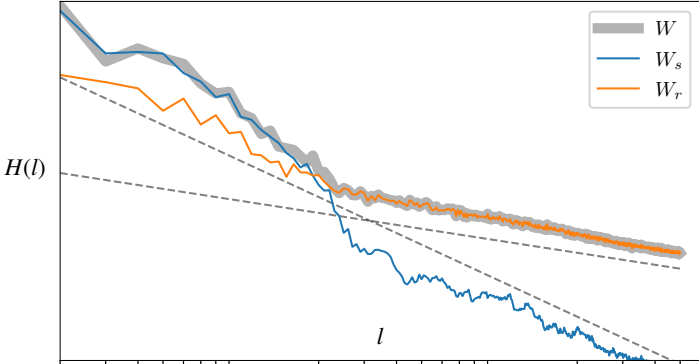


FIG. 9: Energy spectrum in log-log scale for W , W_s , and W_r at $t = t_{end}$ for the simulation where three blobs emerge. The dashed lines indicate the slopes l^{-3} and l^{-1} .

Assumption 1. Let $\psi \in C^1(\mathbb{S}^2)$ be the stream function. Then the critical points of ψ define a set of zero Lebesgue measure on \mathbb{S}^2 , such that it is never dense in any neighbourhood of one of its points.

We say that ψ is *generic* whenever it satisfies Assumption 1. Let us now consider some $f \in C^1(\mathbb{S}^2)$. We see from this definition that $f \in \text{stab}_\psi$ if and only ∇f and $\nabla \psi$ are parallel. Since we take ψ to be generic, the points where $\nabla \psi = 0$ lie on a set

of zero measure, nowhere dense. Therefore, since f is continuous, $f \in \text{stab}_\psi$ if it is constant on the connected components of the level curves of ψ . Then the projection of f onto stab_ψ can be defined by evaluating f on the level curves of ψ , i.e., the streamlines. Let γ be a connected component of a streamline, then we define the projector $\Pi_\psi : C^1(\mathbb{S}^2) \rightarrow \text{stab}_\psi$ as:

$$\Pi_\psi(f)|_\gamma = \frac{1}{\text{length}(\gamma)} \int_\gamma f ds. \quad (9)$$

In the limit case, when γ is a point, clearly $\Pi_\psi(\omega)|_\gamma = f(\gamma)$. We notice that the operator Π_ψ does not preserve in general the continuity of f . Indeed, let us call a point $x \in \mathbb{S}^2$ a *bifurcation saddle point* if x is a saddle point of ψ such that the streamline passing through x contains a bifurcation point. We then have the following result.

Proposition 1. *Let ψ be generic and Π_ψ the projector as defined in (9). Then, if $x \in \mathbb{S}^2$ is a bifurcation saddle point for ψ , there exists $f \in C^1(\mathbb{S}^2)$, such that $\Pi_\psi(f)$ is discontinuous at the streamline passing through x . Vice versa, given $f \in C^1(\mathbb{S}^2)$, if $\Pi_\psi(f)$ is discontinuous at some point $x \in \mathbb{S}^2$, then the streamline passing through x contains a bifurcation saddle point.*

Proof sketch. The issue about the continuity of f can be treated locally. Hence, let us work in Cartesian coordinates. Let $x \in \mathbb{S}^2$ be a bifurcation saddle point for ψ and γ the streamline passing through x . Then, let β be a curve intersecting γ only in x and let f be a smooth function positive at one side of β and negative at the other one, such that $\int_\gamma f ds = 0$. Then being x a bifurcation point, for any neighbourhood U of x , there exist streamlines totally contained in one or another side of β . Then, the average of f on those streamlines is either strictly positive or negative, creating a discontinuity at γ .

Vice versa, let $f \in C^1(\mathbb{S}^2)$, such that $\Pi_\psi(f)$ is discontinuous at some point $x \in \mathbb{S}^2$. Then, the streamline passing through x cannot be homomorphic to any of those in some tubular neighbourhood. Hence, the streamline passing through x must contain a critical point for ψ , which also is a bifurcation saddle point. \square

However, we have the following regularity for Π_ψ .

Proposition 2. *The operator Π_ψ can be extended to a bounded operator with norm one on $L^p(\mathbb{S}^2)$, for every $p \in [1, \infty]$.*

Proof. Let us first notice that Π_ψ is defined from $C^0(\mathbb{S}^2)$ to $L^1(\mathbb{S}^2)$, and satisfies $\|\Pi_\psi f\|_{L^1} \leq \|f\|_{L^1}$, for any $f \in C^0(\mathbb{S}^2)$. Since $C^0(\mathbb{S}^2)$ is dense in $L^1(\mathbb{S}^2)$, it is possible to extend Π_ψ to a bounded operator on $L^1(\mathbb{S}^2)$. Secondly, Π_ψ is well defined from the space of simple functions to $L^\infty(\mathbb{S}^2)$, and satisfies $\|\Pi_\psi f\|_{L^\infty} \leq \|f\|_{L^\infty}$, for any f simple. Since the space of simple functions is dense in $L^\infty(\mathbb{S}^2)$, it is possible to extend Π_ψ to a bounded operator on $L^\infty(\mathbb{S}^2)$. Furthermore, since Π_ψ fixes the constant functions, it must be that $\|\Pi_\psi\|_{L^1} = \|\Pi_\psi\|_{L^\infty} = 1$. Hence, by the Riesz-Thorin theorem, we conclude that $\|\Pi_\psi\|_{L^p} = 1$, for any $p \in [1, \infty]$. \square

Hence, from now on, let us consider equations (8) in the weak form, for $\omega \in L^\infty(\mathbb{S}^2)$. It is clear that $\Pi_\psi^2 = \Pi_\psi$. Moreover, we can formally define the operator Π_ψ via the kernel

$$K(x, y) = \frac{1}{\text{length}(\gamma_x)} \delta_{\gamma_x}(y), \quad \text{for any } x, y \in \mathbb{S}^2$$

where γ_x is the connected component of the streamline passing through x . In this way we get that Π_ψ is self-adjoint with respect to the L^2 inner product, i.e., for any $f, g \in C^\infty(\mathbb{S}^2)$

$$\begin{aligned} \int_{\mathbb{S}^2} f \Pi_\psi g &= \int_{\mathbb{S}^2} f(x) \int_{\mathbb{S}^2} K(x, y) g(y) dy dx \\ &= \int_{\mathbb{S}^2} g(y) \int_{\mathbb{S}^2} K(x, y) f(x) dx dy \\ &= \int_{\mathbb{S}^2} g \Pi_\psi f. \end{aligned}$$

Then, by extension we get the same equalities hold for any $f, g \in L^p(\mathbb{S}^2)$, for any $p \in [1, \infty]$.

Remark 3. We notice that the operator Π_ψ , defined by the kernel $K(x, y)$, is an example of the so called *mixing operators* (or polymorphisms or bistochastic operators), as introduced by [Shnirelman \(1993, 2012\)](#). In those works, the stationary flows are characterized as *minimal elements* accordingly to the partial order on $L^2(\mathbb{S}^2)$ given by: for any $f, g \in L^2(\mathbb{S}^2)$, $f \preceq g$ if and only if there exist a mixing operator, defined via the kernel K , such that $f = K * g$. We will see that this is equivalent to say that a vorticity $\omega \in L^\infty(\mathbb{S}^2)$ satisfies $\Pi_\psi \omega = \omega$. Hence, the stationary flows of the Euler equations correspond to the fixed vorticity of Π_ψ .

We now have the following proposition:

Proposition 3. *Let $f \in L^\infty(\mathbb{S}^2)$ and ψ be generic. Then $f \in \text{stab}_\psi$ if and only if $\Pi_\psi f = f$.*

Proof. Let us prove the result for $f \in C^1(\mathbb{S}^2)$, and conclude by extension. Let $f \in \text{stab}_\psi$. Then, ∇f is parallel to $\nabla \psi$ almost everywhere. Hence, the gradient of f along any streamline must vanish, and so on each connected component it is constant. By continuity of f we deduce that f must be constant also on the streamlines containing some critical points. Therefore, $\Pi_\psi(f) = f$.

Let us now assume that $\Pi_\psi(f) = f$. Then, f must be constant on each connected component of a streamline. Hence, ∇f is orthogonal to the streamlines. Since, $\nabla \psi$ is also orthogonal to the streamlines, we conclude that $\{f, \psi\} = 0$ and so f is in stab_ψ . \square

We are now in position to derive classical analogs of the results in [section III](#) (which were based on the quantized equations). First of all, recall that the stream function ψ satisfies the equation

$$\dot{\psi} = \Delta^{-1}\{\psi, \Delta\psi\}. \quad (10)$$

Equation (10) is not Hamiltonian, but we can split the right hand side into a Hamiltonian and non-Hamiltonian part, using the projection Π_ψ :

$$\dot{\psi} = \Pi_\psi^\perp \Delta^{-1}\{\psi, \Delta\psi\} + \Pi_\psi \Delta^{-1}\{\psi, \Delta\psi\}.$$

Analogously to the quantized case, we would like to find a generator for part $\Pi_\psi^\perp \Delta^{-1}\{\psi, \Delta\psi\}$. In particular, we would like to find a function b such that

$$\{b, \psi\} = \Pi_\psi^\perp \Delta^{-1}\{\psi, \Delta\psi\}. \quad (11)$$

It is clear that a necessary condition for the equation $\{b, \psi\} = f$ to have a solution b is that $f \in \text{stab}_\psi^\perp$. Indeed, if $b \in C^1(\mathbb{S}^2)$ then $\{b, \psi\} \in \text{stab}_\psi^\perp$ since

$$\int_{\mathbb{S}^2} \{b, \psi\} g = - \int_{\mathbb{S}^2} \{g, \psi\} b = 0 \quad \text{for any } g \in \text{stab}_\psi.$$

However, in general equation (11) can be solved only where $\nabla \psi \neq 0$. Around the critical points of ψ the gradient of b is potentially unbounded. Moreover, the right hand side in equation (11) can be discontinuous at the level curves of ψ containing saddle points of ψ . Hence, b can only be defined almost everywhere. Furthermore, we have the following:

Proposition 4. *Let $f \in C^0(\mathbb{S}^2)$ and ψ be generic. Then $f \in \text{stab}_\psi^\perp$ if and only if there exists b almost everywhere smooth, such that $\{b, \psi\} = f$ on the set $\nabla \psi \neq 0$.*

Proof. The if part is clear. Let instead take $f \in \text{stab}_\psi^\perp$. Then, for any point $x \in \mathbb{S}^2$, we have to solve the PDE for b :

$$\nabla^\perp \psi \cdot \nabla b = f, \quad (12)$$

where $\nabla^\perp \psi = x \times \nabla \psi$. If $\nabla \psi$ does not vanish, equation (12) can be solved by integration in the direction of $\nabla^\perp \psi$. In the points where $\nabla \psi$ does not vanishes, ∇b is not defined by equation (12), and it can be unbounded around those points. Hence, the field b is almost everywhere smooth and satisfies $\{b, \psi\} = f$, where $\nabla \psi \neq 0$. \square

In order to derive the dynamical equations for ω_s , we cannot use directly the field b . Instead, we consider the volume preserving vector field

$$X[\psi] := \Pi_\psi^\perp \Delta^{-1}\{\psi, \Delta\psi\}.$$

We note that X corresponds to the infinitesimal action of a map φ_t which transports ψ by deforming its level curves. Hence, φ_t acts naturally on stab_ψ . Let us write Π_t^ψ for the projection onto stab_ψ at time t . Then, for any point $x \in \mathbb{S}^2$, let

$$\gamma(t) = \{y \mid \psi(y) = \psi(x) \text{ and } y \text{ in connected component of } x\},$$

and $d\hat{s}_t$ the normalized Lebesgue measure on $\gamma(t)$. We have then the formal identity

$$\begin{aligned} \omega_s(t, x) &= \Pi_t^\psi \omega(t, x) \\ &= \int_{\gamma(t)} \omega(t, y) d\hat{s}_t(y) \\ &= \int_{\gamma(0)} (\varphi_t^* \omega)(t, y) d\hat{s}_0(y) \\ &= \Pi_\psi^0 (\varphi_t^* \omega)(t, \varphi_t^{-1}(x)). \end{aligned}$$

Hence, for any test function $\phi \in C^\infty(\mathbb{S}^2)$

$$\begin{aligned} \frac{d}{dt} \int_{\mathbb{S}^2} \omega_s(t, x) \phi(x) &= \frac{d}{dt} \int_{\mathbb{S}^2} \Pi_\psi^0(\varphi_t^* \omega)(t, \varphi_t^{-1}(x)) \phi(x) \\ &= \int_{\mathbb{S}^2} \left(\Pi_\psi^0(\varphi_t^* \mathcal{L}_X \omega)(t, \varphi_t^{-1}(x)) - \mathcal{L}_X \Pi_\psi^0(\varphi_t^* \omega)(t, \varphi_t^{-1}(x)) \right) \phi(x) \\ &= - \int_{\mathbb{S}^2} \omega(t, x) \mathcal{L}_X \Pi_\psi^t \phi(x) + \mathcal{L}_X \Pi_\psi^t \omega(t, x) \phi(x) \end{aligned}$$

where \mathcal{L}_X is the Lie derivative, which simply acts on functions as $\mathcal{L}_X f = X[f]$. We notice from the previous calculations that \mathcal{L}_X has to be evaluated only on elements in stab_ψ . Hence, the time derivative of ω_s is well defined in the weak sense.

Let us now formally denote $X := -\{b, \cdot\}$. Then, interpreting the Poisson bracket in the weak sense, we can write the dynamical system for ω_s, ω_r as:

$$\begin{aligned} \dot{\omega}_s &= \{b, \omega_s\} - \Pi_\psi \{b, \omega_r\} \\ \dot{\omega}_r &= -\{b, \omega_s\} + \Pi_\psi \{b, \omega_r\} + \{\psi, \omega_r\} \\ \{b, \psi\} &= \Pi_\psi^\perp \Delta^{-1} \{\psi, \omega_r\}, \end{aligned}$$

where b is implicitly defined by the third equation and $\psi = \Delta^{-1}(\omega_s + \omega_r)$. We notice that the equations of motion for ω_s can also be written in a more compact form as:

$$\dot{\omega}_s = [\Pi_\psi, \mathcal{L}_X] \omega,$$

where the square bracket is a commutator of operators.

Finally, we notice that the energy and enstrophy splitting is valid also in the classical setting:

$$\begin{aligned} H(\omega) &= H(\omega_s) - H(\omega_r) \\ E(\omega) &= E(\omega_s) + E(\omega_r). \end{aligned}$$

VI. CONCLUSIONS AND OUTLOOK

Based on the quantized Euler equations we have reported on a new technique for studying 2D turbulence via the canonical splitting of vorticity. By numerical simulations and some theoretical evidence, this splitting dynamically develops into a separation of scales. We have further presented a weak L^∞ mathematical foundation for the theory in the classical setting.

As the numerical simulations so strikingly captures the scale separation process, and as the inverse relations of the corresponding energy-enstrophy splitting reflect the stationary theory of Kraichnan, it is likely that further numerical and theoretical studies of the canonical vorticity splitting shall unveil more details on the mechanism behind vortex condensation. Furthermore, the splitting into large scales ω_s and small scales ω_r suggests to use these variables as a basis for *stochastic model reduction* (cf. [Jain et al. \(2015\)](#)) of the two-dimensional Euler equations, with ω_r modelled as multiplicative noise.

APPENDIX A: STREAM FUNCTION SPLITTING

In this section, we present the analogous splitting of Section III for the stream function P . Let stab_W be the stabilizer

of W in $\mathfrak{su}(N)$. Then, we can consider the stream function splitting $P = P_s + P_r$, where P_s is the orthogonal projection of P onto stab_W , and P_r the orthogonal complement. Similarly to what we have done in Section III, P_s can be constructed by finding U unitary which diagonalizes W :

$$U^* W U = D,$$

and then defining $P_s = U \text{diag}(U^* W U) U^*$. By definition the quantized Euler equations for the stream function P can be written as:

$$\dot{P} = \Delta_N^{-1} [P_r, \Delta(P_s + P_r)],$$

the energy $H(P) = \frac{1}{2} \text{Tr}(\Delta_N(P_s + P_r)P_s) = \frac{1}{2} \text{Tr}(\Delta_N(P_s)P_s) - \frac{1}{2} \text{Tr}(\Delta_N(P_r)P_r)$ and the enstrophy $E(P) = -\text{Tr}((\Delta_N(P_s + P_r))^2)$. Notice that the enstrophy $E(P) = -\text{Tr}((\Delta_N P)^2)$, in the P_s, P_r does not admit a splitting contrary to the energy $H(P) = \text{Tr}(\Delta_N P P)$:

$$\begin{aligned} H(P) &= H(P_s) - H(P_r) \\ E(P) &\neq E(P_s) + E(P_r). \end{aligned}$$

Since the eigenvalues of W are constant in time, the dynamics of P_s, P_r variables is simpler than the one of W_s, W_r . In fact, we have that $\dot{U}U = P$ and so

$$\begin{aligned} \dot{P}_s &= [\dot{U}U, P_s] - \Pi_W[\dot{U}U, P_r] + \Pi_W(\dot{P}) \\ &= [P_r, P_s] + \Pi_W(\Delta_N^{-1} [P_r, \Delta_N(P_s + P_r)]), \end{aligned}$$

and

$$\dot{P}_r = -[P_r, P_s] + \Pi_W^\perp(\Delta_N^{-1} [P_r, \Delta_N(P_s + P_r)]).$$

To understand how the dynamics of the P_s, P_r variables look, we consider the first numerical simulation of Section IV. In Figure 10 the three stream function fields P, P_s, P_r are shown at the times $t = 0$ and $t = t_{\text{end}}$. We notice that from a very smooth P , the projection Π_W onto the stabilizer rougher field W produce a much coarser image. In particular, both P_s and P_r do not show any additional structure or scale separation unlike to W_s and W_r .

REFERENCES

- Abramov, R. V., and A. J. Majda (2003), Proc. Nat. Acad. Sci. (USA) **100** (7), 3841.
- Arnold, V. I., and B. A. Khesin (1998), *Topological Methods in Hydrodynamics* (Springer-Verlag, New York).
- Boffetta, G., and R. E. Ecke (2012), *Annu. Rev. Fluid Mech.* **44** (1), 427.
- Bordemann, M., E. Meinrenken, and M. Schlichenmaier (1994), Comm. Math. Phys. **165** (2), 281.
- Bouchet, F., and A. Venaille (2012), Physics reports **515** (5), 227.
- Caglioti, E., P. L. Lions, C. Marchioro, and M. Pulvirenti (1992), Comm. Math. Phys. **143** (3), 501.
- Caglioti, E., P. L. Lions, C. Marchioro, and M. Pulvirenti (1995), Comm. Math. Phys. **174** (2), 229.

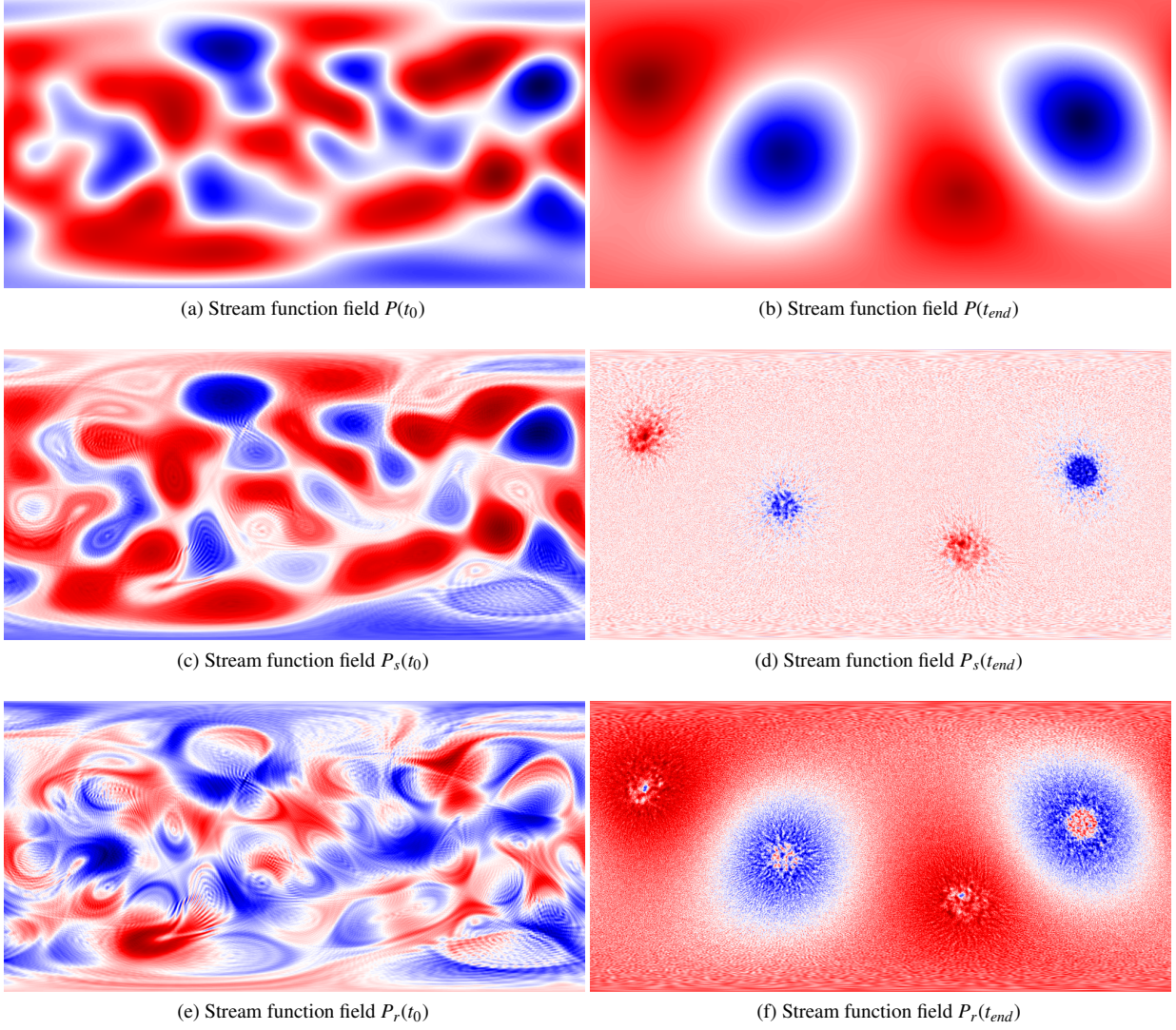


FIG. 10: The Stream function fields fields P, P_s, P_r at $t = 0$ and $t = t_{end}$.

- Chertkov, M., C. Connaughton, I. Kolokolov, and V. Lebedev (2007), *Phys. Rev. Lett.* **99**, 084501.
- Couder, Y. (1984), *Journal de Physique Lettres* **45** (8), 353.
- Cullen, M. J. P. (2006), *A Mathematical Theory of Large-Scale Atmosphere/Ocean Flow* (Imperial College Press).
- Dolzansky, F. V. (2013), *Fundamentals of geophysical hydrodynamics*, Vol. 103 (Springer).
- Dritschel, D., W. Qi, and J. Marston (2015), *J. Fluid Mech.* **783**, 1.
- Euler, L. (1757), *Académie Royale des Sciences et des Belles-Lettres de Berlin, Mémoires* **11**, 217.
- Eyink, G. L., and K. R. Sreenivasan (2006), *Rev. Mod. Phys.* **78** (1), 87.
- Farge, M., K. Schneider, and N. Kevlahan (1999), *Phys. Fluids* **11** (8), 2187.
- Gauthier, G., M. T. Reeves, X. Yu, A. S. Bradley, M. A. Baker, T. A. Bell, H. Rubinsztein-Dunlop, M. J. Davis, and T. W. Neely (2019), *Science* **364** (6447), 1264.
- Herbert, C. (2013), *J. Stat. Phys.* **152** (6), 1084.
- Hoppe, J., and S.-T. Yau (1998), *Comm. Math. Phys.* **195**, 66.
- Jain, A., I. Timofeyev, and E. Vanden-Eijnden (2015), *Commun. Math. Sci.* **2** (13), 297.
- Johnstone, S. P., A. J. Groszek, P. T. Starkey, C. J. Billington, T. P. Simula, and K. Helmerson (2019), *Science* **364** (6447), 1267.
- Kiessling, M. K.-H. (1993), *Comm. Pure Appl. Math.* **46** (1), 27.
- Kirillov, A. A. (2004), *Lectures on the orbit method*, Vol. 64 (American Mathematical Soc.).
- Kolmogorov, A. N. (1941), in *Dokl. Akad. Nauk SSSR*, Vol. 30, pp. 299–303.
- Kraichnan, R. H. (1967), *Phys. Fluid.* **10** (7), 1417.
- Kraichnan, R. H. (1975), *J. Fluid Mech.* **67** (1), 155.
- Kuksin, S., and A. Shirikyan (2012), *Mathematics of two-dimensional turbulence* (Cambridge University Press).
- Kuksin, S., and A. Shirikyan (2017), *Phys. Fluids* **29** (12), 125106.
- Majda, A., and X. Wang (2006), *Nonlinear Dynamics and Statistical Theories for Basic Geophysical Flows* (Cambridge University Press).
- Marchioro, C., and M. Pulvirenti (2012), *Mathematical theory of incompressible nonviscous fluids*, Vol. 96 (Springer Science & Business Media).

- McLachlan, R. (1993), Phys. Rev. Lett. **71** (19), 3043.
- Miller, J. (1990), Phys. Rev. Lett. **65**, 2137.
- Modin, K., and M. Viviani (2020a), J. Fluid Mech. **884**, A22.
- Modin, K., and M. Viviani (2020b), Arnold Math. J..
- Modin, K., and M. Viviani (2020c), Found. Comput. Math. **20**, 889.
- Nastrom, G. D., K. S. Gage, and W. H. Jasperson (1984), Nature **310** (5972), 36.
- Onsager, L. (1949), Il Nuovo Cimento (1943-1954) **6** (2), 279.
- Pedlosky, J. (2013), *Geophysical fluid dynamics* (Springer).
- Robert, R., and J. Sommeria (1991), J. Fluid Mech. **229**, 291–310.
- Schlichenmaier, M. (2001), Ser Con Appl Math.
- Shnirelman, A. (1993), Russ. J. Math. Phys **1** (1), 105.
- Shnirelman, A. (2012), Procedia IUTAM , 151.
- Sommeria, J. (1988), J. Fluid Mech. **189**, 553.
- Xiao, Z., M. Wan, S. Chen, and G. L. Eyink (2009), J. Fluid Mech. **619**, 1.
- Yudovich, V. I. (1963), Zh. Vychisl. Mat. Mat. Fiz. **3** (6), 1032.
- Zeitlin, V. (1991), Phys. D **49** (3), 353.
- Zeitlin, V. (2004), Phys. Rev. Lett. **93** (26), 353.
- Zeitlin, V. (2018), *Geophysical fluid dynamics: understanding (almost) everything with rotating shallow water models* (Oxford University Press).